

Lawrence Berkeley National Laboratory

Recent Work

Title

Design Strategies for Monolithic Adjustable-Radius Metal Mirrors

Permalink

<https://escholarship.org/uc/item/0s4653jj>

Journal

Optical Engineering, 34(2)

Author

Howells, M.R.

Publication Date

1994-08-05



Lawrence Berkeley Laboratory

UNIVERSITY OF CALIFORNIA

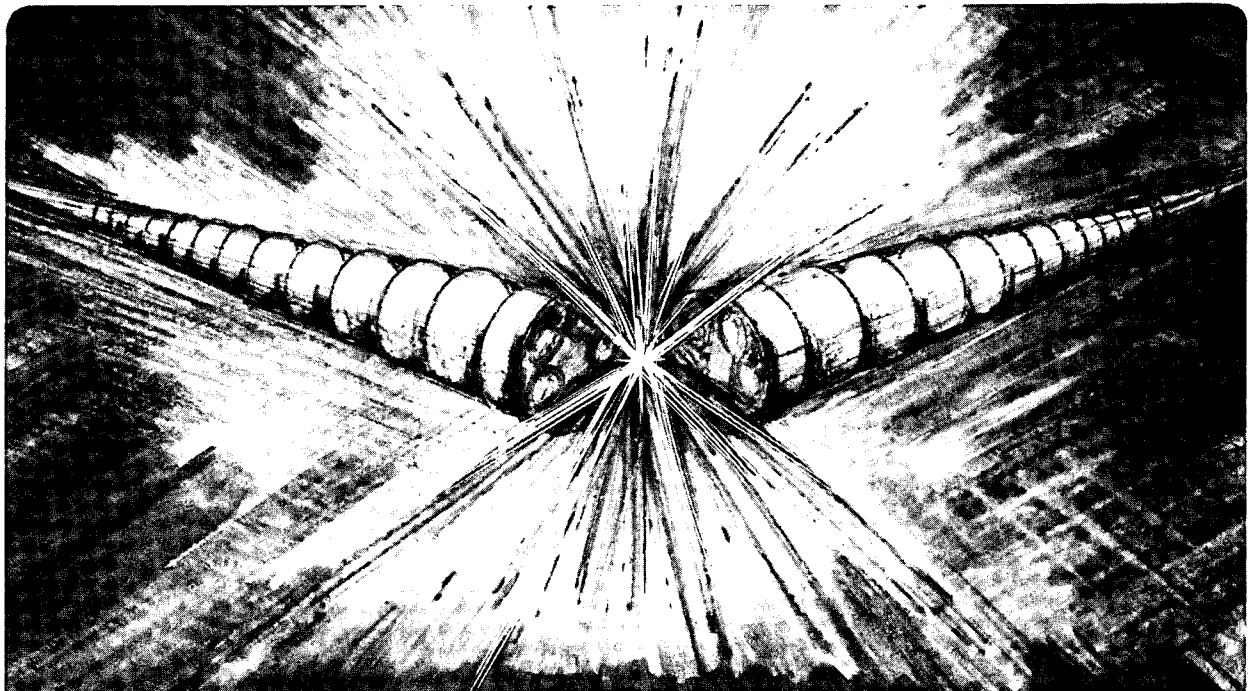
Accelerator & Fusion Research Division

Submitted to Optical Engineering

Design Strategies for Monolithic Adaptive Metal Mirrors

M. Howells

August 1994



REFERENCE COPY
Does Not
Circulate

Copy 1

LBL-35977

DISCLAIMER

This document was prepared as an account of work sponsored by the United States Government. While this document is believed to contain correct information, neither the United States Government nor any agency thereof, nor the Regents of the University of California, nor any of their employees, makes any warranty, express or implied, or assumes any legal responsibility for the accuracy, completeness, or usefulness of any information, apparatus, product, or process disclosed, or represents that its use would not infringe privately owned rights. Reference herein to any specific commercial product, process, or service by its trade name, trademark, manufacturer, or otherwise, does not necessarily constitute or imply its endorsement, recommendation, or favoring by the United States Government or any agency thereof, or the Regents of the University of California. The views and opinions of authors expressed herein do not necessarily state or reflect those of the United States Government or any agency thereof or the Regents of the University of California.

DESIGN STRATEGIES FOR MONOLITHIC ADAPTIVE METAL MIRRORS*

M. Howells

Advanced Light Source
Accelerator and Fusion Research Division
Lawrence Berkeley Laboratory
University of California
Berkeley, CA 94720

August 1994

Paper invited by Optical Engineering

*This work was supported by the Director, Office of Energy Research, Office of Basic Energy Sciences, Materials Sciences Division, of the U.S. Department of Energy, under Contract No. DE-AC03-76SF00098.

DESIGN STRATEGIES FOR MONOLITHIC ADAPTIVE METAL MIRRORS

Malcolm R. Howells,

Advanced Light Source, Lawrence Berkeley Laboratory, Berkeley CA 94720, USA.

ABSTRACT

The design principles and special advantages of monolithic adaptive metal mirrors have been described in an earlier paper¹. The present paper provides analysis for understanding the response of such mirrors to the unintended torques they receive from the flexural hinges which connect them to the bending system. The analysis includes mirrors both with and without water-cooling channels. The torsional rigidities of the usual types of flexural hinge and of the most common mirrors are calculated thus allowing the hinge-induced distortions of any mirror surface to be estimated. Two strategies for reducing such errors are proposed. One involves the design of sufficiently flexible hinges and the other the elimination of the hinge rotations (and therefore their torques) altogether by means of a new design principle. Some analysis of the latter scheme is provided including a prescription for choosing suitable design parameters.

KEY WORDS

Grazing-incidence mirrors, adaptive optics, flexural hinges, x-ray focusing, high-power mirrors

1.0 INTRODUCTION

Monolithic adaptive mirrors for grazing incidence applications can be cut from a single block of metal using a wire, electric discharge machining (EDM) system. The cut shape is designed to act as a single flexural mechanism comprising both the mirror and its bending device. This type of all-metal component is particularly well-suited for grazing-incidence x-ray mirrors for synchrotron radiation beam lines and is compatible with intensive water-cooling arrangements. In an earlier paper¹ we have described the principles of monolithic design and its advantages for mirror systems as well as the theory that allows one to achieve prescribed mirror shapes by means of a controlled variation of the mirror thickness with position. The ideas in reference 1 have already been applied successfully to a number of mirrors manufactured commercially by Rockwell Power Systems² and Photon Sciences International³. The above paper also provides a number of references describing earlier work on adaptive x-ray mirrors. The closest antecedent to the monolithic schemes considered here is the mirror described by Ice et al⁴ which is a water-cooled metal mirror bent into a circular shape by a single point load. In the present paper we continue the treatment of the theory of adaptive monolithic mirrors paying special attention to the effects of the three hinges which together provide the force system which deforms the mirror.

In reference 1 we discussed the design shown in Fig. 1 which would, for example, provide a circular reflecting surface if the mirror thickness were made proportional to the cube root of the distance from the end. The mirror is bent by applying a point load in the center and the circular shape will be good over the region where the cube root law is obeyed provided that the assumptions of beam theory are satisfied⁵ and that the three narrow webs of material linking the mirror to the bending mechanism behave as perfect (torque-free) hinges. In the earlier paper we also discussed the consequences of having a non-zero torque at the center hinge which would apply an unwanted moment to the mirror at its center leading to a corresponding twist ("S"-shaped error) of the mirror surface. Torque by the center hinge is potentially more harmful than by the end ones but it is eliminated in the design of Fig. 1 by the

rectangle mechanism *fghi*. The latter ensures that the rigid member *ej* moves up or down without rotation so that the "hinge" at *e* never rotates and thus never torques the mirror.

Although the design of Fig. 1 has been used quite successfully, it continues to have the weakness that the two hinges at the ends do rotate as the mirror bends and therefore they do torque the mirror and cause small distortions ("M" or "W" shaped errors). Moreover the size of this error appears to be such that it could be a barrier to achieving microradian or submicroradian accuracy on mirrors fabricated by monolithic bending techniques. In view of the practical importance of the problem and the fact that we believe we have solutions to it, we consider the question of the distorting effect of the hinges on the mirror in more detail in this paper.

In schemes such as that of Fig. 1, in which some of the hinges rotate, the strategy must be to arrive at a hinge design with a sufficiently low torsional rigidity (torque per unit angle) that the resulting mirror distortions are within tolerance. This is the simplest approach and, on present experience, seems to be satisfactory down to about 0.5-1 arc second tolerances at moderate curvatures (>100m radius, say). However, we believe that this design principle has not yet been carried to its limit.

To implement such an approach requires an understanding of the torsional rigidities of both the mirror and the hinges and of the stresses that will develop. We provide a treatment of the torsional rigidity of mirrors in section 2 including those with a uniform section and those with a cube-root thickness variation both with and without cooling channels. In section 3 we describe the torsional properties of the types of flexural hinges normally used in monolithic mirrors and in section 4 we show how the mirror performance depends on the relative sizes of the torsional rigidities of the hinge and the mirror.

To do better than this and to deal with cases where we expect a large bending force or a large amount of bend, which implies thicker hinges and greater hinge torques, we need a new design principle. We need to develop a design in which all three hinges that connect to the mirror have zero rotation and thus apply zero (unintended) torque to the mirror. We have developed such a design and give a description and analysis of it in section 5.

2.0 DISTORTION OF A MIRROR BY APPLICATION OF COUPLES

We will analyze the mirrors and hinge types of interest using standard beam theory. The validity conditions for such an analysis have been discussed by Roark⁵ and although the conditions are usually well satisfied by adaptive mirrors this is not generally the case for the hinges linking the mirror to the driver. Nevertheless we will proceed to use beam theory for both and defer till later the question of its validity for hinges.

2.1 *Twisting of a uniform mirror at its center*

The general equation of beam theory is

$$YI(x) \frac{d^2y}{dx^2} = M(x) \quad (1)$$

where Y is the Young's modulus, I the section moment of inertia and M the bending moment (see Fig. 2a). For a rectangular section of height h , and width b , $I=bh^3/12$. We consider first the case of a mirror of uniform cross section with fixed ends, subjected to a torque C at its center. For this case we have $I(x)=I_0=\text{constant}$ and $M(x)=(L/2-x)C/L$. Integrating (1) twice and applying the boundary conditions $(y)_{x=0}=0$ and $(y)_{x=L/2}=0$, we arrive at the following equation for the slope

$$YI_0 \frac{dy}{dx} = \frac{Cx}{2} - \frac{Cx^2}{2L} - \frac{CL}{12} \quad (2)$$

from which we can conclude that the torsional rigidity of the mirror (τ_{um}) is given by

$$\tau_{um} = \frac{C}{\left. \frac{dy}{dx} \right|_{x=0}} = \frac{12YI_0}{L} \quad (3)$$

2.2 Twisting of a "cube-root" mirror at its center

For a cube-root mirror we have

$$I(x) = \frac{2I_0}{L} \left(\frac{L}{2} - x \right) \quad (4)$$

So using the same $M(x)$ as before and substituting it and (4) into (1) we find that the equation simplifies to

$$2YI_0 \frac{d^2y}{dx^2} = C \quad (5)$$

where I_0 now refers specifically to $I(0)$. The constant bending moment indicates constant curvature meaning that the twist at the center will produce two circular curves of opposite sense. (5) leads similarly to an expression for the torsional rigidity τ_{cm} of the center of a cube-root mirror.

$$\tau_{cm} = \frac{8YI_0}{L} \quad (6)$$

2.3. Twisting of a uniform mirror at both ends

For a monolithic mirror one usually has a strongly constrained symmetrical situation where the center and the ends of the mirror are maintained in definite positions by the bending forces. If we superpose on that the hinge torques at the ends and consider only the errors produced by such torques then we can take the boundary conditions to be

$$y|_{x=0} = \left. \frac{dy}{dx} \right|_{x=0} = y|_{x=L/2} = 0 \quad (7)$$

and compute the value of $C/(dy/dx)_{x=L/2}$ as before. The extra boundary condition is needed to calculate the forces on the mirror since for this case the forces depend on the elastic properties of the mirror and cannot be determined from statics. The result is

$$\tau_{ume} = \frac{8YI_0}{L} \quad (8)$$

2.4. Twisting of a composite mirror at both ends

The most realistic case for our purposes is a constrained cube root mirror which has a small section of length ΔL at each end with constant thickness (see Fig. 1 for example). One reason for including such a straight section is to allow cooling channels to enter and leave through the ends of the mirror. The situation is again "statically indeterminate" and we proceed using the same boundary conditions (equation (7)) as before to

$$\tau_{compe} = \frac{\frac{2YI_0}{L}}{\frac{6(1-x)^2}{3-4x^2} + \ln(2x) - 1} \quad (9)$$

where $x=\Delta L/L$. The conclusion of the calculation expressed in equation (9) is that τ_{compe} is slightly higher than the torsional rigidity of a similarly constrained uniform mirror of thickness equal to the end thickness of the composite mirror. This is reasonable and if we take as an example an end thickness of half the center thickness, we find that

$$\frac{\Delta L}{L} = \frac{1}{16} \quad \frac{\tau_{compe}}{\tau_{ume}} = 1.524 \quad (10)$$

2.6. Effect of cooling channels on the torsional properties of mirrors

The control of the shape of the type of adaptive mirrors we are considering here depends on being able to program $I(x)$, the moment of inertia of the cross section area of the mirror to any desired value. Naturally if the mirror has cooling channels, the shape of the cross section area is modified and the section moment is reduced. To deal with this we propose to increase the thickness, $h(x)$, at each position along the mirror length to that value which restores $I(x)$ to its original value (before cooling channels were introduced). Once we have calculated the new form of h , the EDM machine can be programmed to cut that form as easily as any other.

In calculating the consequences of cooling channels we adopt a general method which applies to the removal of any shape or shapes from the initially rectangular cross section. This includes in particular, circular or rectangular cooling channels and the portion of a circle removed when a concave cylinder is ground into a flat mirror blank. Remembering that $I(x)$ must be calculated relative to the neutral axis and that this shifts when the shape of the section changes, we proceed as follows:

Let the i th shape to be removed have area A_i and center of gravity distant s_i from the mirror surface. Let h be the new thickness value that will restore the section moment to the value $I=bh(x)^3/12$ that prevailed before the shapes were removed. Taking moments about the new neutral axis (assumed to be distant f from the bottom of the section) we find

$$(h-f)b\frac{h-f}{2} = fb\frac{f}{2} - \sum_i A_i(f-s_i). \quad (11)$$

Now let the moment of inertia of A_i about an axis through its center of gravity parallel to the neutral axes be I_i . Then the equation for h is

$$I_0 = \frac{f^3b}{12} + fb\left(\frac{f}{2}\right)^2 + \frac{(h-f)^3b}{12} + (h-f)b\left(\frac{h-f}{2}\right)^2 - \sum_i (I_i + A_i(f-s_i)^2) \quad (12)$$

In arriving at (12) we have used the parallel-axis theorem which states that if the moment of inertia of an area A is I_G about an axis through the center of gravity and I about a parallel axis displaced by z , then $I=I_G+Az^2$. Collecting terms we get

$$I_0 = \frac{b}{3}h^3 + f^2(bh-P) - 2f\left(\frac{h^2b}{2} - Q\right) - R - S \quad (13)$$

where

$$P = \sum_i A_i; \quad Q = \sum_i A_i s_i; \quad R = \sum_i A_i s_i^2; \quad S = \sum_i I_i$$

According to (11)

$$f = \frac{\frac{h^2b}{2} - Q}{hb - P} \quad (14)$$

so substituting for f in (13) we finally get

$$\left(\frac{bh^3}{3} - R - S - I_x\right)(bh - P) - \left(\frac{h^2b}{2} - Q\right)^2 = 0 \quad (15)$$

which is a quartic in h with everything else known. The correct solution is the one which is slightly greater than the original value of $h(x)$.

3.0 TWISTING OF FLEXURAL HINGES

3.1. Torsional rigidity of a double-sided notch hinge

The most useful type of flexural hinges for monolithic mirror designs are the so-called "notch" hinges made by drilling two circular holes or a hole and a straight edge close to each other (Fig. 2b, 2c). We now apply the above type of theory to this hinge which is assumed to be loaded by a pure torque. For the case illustrated in Fig. 2b, using equation (1) and $I(x)=bh^3/12$, we arrive first at the differential equation

$$\frac{d^2y}{dx^2} = \frac{12C}{bY} \frac{1}{\left[2\left(\rho - \sqrt{\rho^2 - x^2}\right) + t\right]^3} \quad (16)$$

The boundary condition is $(dy/dx)_{x=-\rho}=0$ and (9) can be integrated using a standard form⁶ to give the torsional rigidity, $\tau_{hinge}=C/(dy/dx)_{x=\rho}$ as

$$\tau_{hinge} = \frac{bYQ^2}{12\rho \left\{ \frac{1}{a} + \frac{1}{Q^2} \left[a + \frac{8\rho^2}{a} + \frac{12a\rho}{Q} \tan^{-1}\left(\frac{Q}{t}\right) \right] \right\}} \quad (17)$$

where $a=2\rho+t$ and $Q^2=4\rho t+t^2$. Considering the limit $\rho \gg t$, we find that the third term of the square bracket is the dominant one and (17) can be approximated by

$$\tau_{hinge} = \frac{2Ybt^{5/2}}{9\pi\sqrt{\rho}} \quad (18)$$

which agrees with the result of Paros and Weisbord⁷. This expression is widely used and it has been tested⁸ experimentally for two different thickness webs. It gave errors of about 20% for $\rho/t=2.2$ and 3.7.

To simplify the presentation of results we consider the torsional rigidity of the notch hinge in ratio to that of a flat rectangular beam of the same material and identical length, 2ρ , width, b , and center thickness, t . The torsional rigidity of the rectangular-beam hinge is given by

$$\tau_{beam} = \frac{Ybt^3}{24\rho} \quad (19)$$

so that the ratio $G(y)=\tau_{hinge}/\tau_{beam}$ can be calculated from this and equation (17). $G(y)$ can then be expressed as a function of a single variable, the dimensionless shape parameter $y=\rho/t$, as follows

$$G(y) = \frac{\tau_{hinge}}{\tau_{beam}} = \frac{2f^2}{\frac{1}{g} + \frac{1}{f^2} \left(g + \frac{8y^2}{g} + \frac{12gy}{f} \tan^{-1} f \right)}$$

$$f = \sqrt{4y+1}$$

$$g = 2y+1$$
(20)

The expression $G(y)$ is plotted as the continuous curve in Fig. 3. One can see that it approaches unity in the limit $y \rightarrow 0$ as it should and that it increases rather slowly with y . One can also get an approximate expression for $G(y)$ by using the Paros-and-Weisbord approximation for τ_{hinge}

$$G(y) \cong \frac{16}{3\pi} \sqrt{y}$$
(21)

which is also plotted in Fig. 3 and is seen to be a surprisingly good approximation. The analytical results are compared in Fig 3 to two sets of finite element calculations due to Smith⁹ and Andresen¹⁰. It is noteworthy that the agreement is very good, much better than one would expect based on the usual validity conditions of beam theory⁵. This is perhaps due to the fact that only the region close to the center of the hinge (which is the most beam like) actually bends significantly. The most useful conclusion from Fig. 3 is that the Paros-and-Weisbord curve agrees so well with the finite element calculations (at least for $y \geq 1$) that it can be safely used for essentially all design purposes. This conclusion of our analysis of the double-sided notch hinge can thus be summarized in the following very simple form

$$\tau_{hinge} \cong 1.70 \sqrt{y} \tau_{beam}$$
(22)

3.2. Torsional rigidity of a single-sided notch hinge

The single-sided notch hinge is obtained by slicing the double-sided one longitudinally (Fig. 2). Equation (16) then shows that the torsional rigidity of the single-sided hinge is one eighth that of a double-sided hinge of the same radius and twice the center thickness. It seems likely that the single-sided hinge may obey beam theory less well than the double-sided one because the latter but not the former has symmetry about the neutral axis.

3.3. Torsional rigidity of composite hinges

The flat beam is not only of interest as an easy reference for the above calculations but also as a part of the hinge. The combination of a circular and a straight section as shown in Fig. 4 provides a good compromise between the competing requirements for high compressive or tensile strength and low torsional rigidity (i. e. low torque on the mirror). It also reduces the stress concentration which occurs near the center of pure circular hinges by spreading the region of bend. The flat-beam design does lead to a less ideal hinge in the sense of producing a less pure rotation about an axis, but a monolithic mirror does not rely on this aspect of the flexural hinges.

In order to calculate the torsional rigidity of the combined hinge we have only to recognize that torsional rigidities connected in series add harmonically. That is if we join two beams of torsional rigidity τ_1 and τ_2 end to end the torsional rigidity τ_{tot} of the combined beam is given by

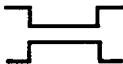




$$\frac{1}{\tau_{tot}} = \frac{1}{\tau_1} + \frac{1}{\tau_2}$$
(23)

Suppose we have a circular hinge with $y=1$ and that we add a straight section of equal length, 2ρ , in the center in the manner of Fig. 4. The torsional rigidity of the circular part would be about $2\tau_{beam}$ from Fig. 3 so from equation (23) the combined torsional rigidity would be $2\tau_{beam}/3$. Similarly if we insert n such sections in the center the combined torsional rigidity would be $2\tau_{beam}/(2n+1)$. This therefore represents a way to reduce the torsional rigidity without reducing the cross section (and thus the strength) which is exactly what we need for the present application. The amount of improvement is shown in Fig. 5.

3.4. Stress in flexural hinges

Another important element in the design of flexural hinges is the stress which for the full-length notch hinges has a maximum at the center. For any beam the local bending stress is given by $Yy'/R = My'/I$ where y' is a y coordinate measured relative to the neutral axis. These expressions for the stress can be evaluated by beam theory from the definitions given in section 2. The maximum stress, and the torsional rigidity of the main hinge shapes used in mirror design are tabulated for reference in Table 1. The torsional rigidity of composite hinges can be found from equation (23).

Table I: Design Formulas for flexural hinges

Element shape	Torsional rigidity	Maximum stress
	$\tau_{beam} = \frac{Ybt^3}{24\rho}$	$\sigma_{beam} = \frac{Yt\theta}{4\rho}$
	$G(y) \tau_{beam}$	$G(y) \sigma_{beam}$
	$\frac{G(2y)}{8} \tau_{beam}$	$\frac{G(2y)}{8} \sigma_{beam}$
	$2G(y) \tau_{beam}$	$2G(y) \sigma_{beam}$
	$\frac{G(2y)}{4} \tau_{beam}$	$\frac{G(2y)}{4} \sigma_{beam}$

All the elements are taken to be of full length 2ρ , width b , and full thickness t except that the quarter-circle ones (which are formed by cutting the

semicircle ones in half) have length ρ . $G(y)$ is given by equation (20) or (21) where $y=\rho/t$.

4.0 APPLICATION TO MIRROR DESIGN

The unwanted angular change θ_{um} (the asymmetric slope error) at the center of a uniform mirror due to a rotation θ_h of the hinge at the center would be

$$\theta_{um} = \theta_h \frac{\tau_{hinge}}{\tau_{um}}. \quad (24)$$

Similarly the angular error at the end of a composite mirror is

$$\theta_{compe} = \theta_h \frac{\tau_{hinge}}{\tau_{compe}} \quad (25)$$

We can see from the expressions for τ_{hinge} and τ_{compe} that the mirror bend angles are independent of Y and b as one might expect. The unintended distortion induced in other types of mirror by hinge torques can be calculated in similar fashion.

Practical choices of values for ρ and t in Glidcop mirrors are 0.25-0.5 mm for ρ and 0.25-1.0 mm for t depending on the forces. The center hinge should have twice the thickness of the end hinges since it carries twice the load. From Fig. 5, one can see that one-to-three diameters of straight section in the center of the hinge is reasonable when there is a need to reduce the stiffness.

Equations (24) and (25) and the earlier theory will often allows us to choose an overall design of mirror and hinges that can keep the hinge-induced distortions below a given tolerance. On the other hand, in cases where this is not possible, we need a new type of design where the hinge torques are *intrinsically* corrected and to this we now turn.

5.0 MONOLITHIC MIRROR DESIGN WITH ZERO UNINTENDED STRESSES

If we bend the mirror in Fig. 1 from flat to a concave radius R_0 then the slope at the end increases from zero to $\theta=\sin^{-1}(L/2R_0)$ (where L is the length of the mirror) and this is the amount by which the end hinges would normally have to rotate. In order to avoid hinge rotation altogether for the hinge at c in Fig. 1, we would need to rotate the rigid member cd anti clockwise from 0 to θ in synchronism with driving the curvature of the mirror from zero to $1/R_0$. The member ab would have to rotate similarly but in the opposite direction. Our proposed mechanism to accomplish this is shown in Fig. 6. It is drawn with maximum symmetry for clarity although, in practice, the base member would normally be much thicker than the mirror. The primary element of the flexure is a rhombus with four rigid members A"C', C"B', B"D' and D"A'. When the mirror is deformed from flat toward concave this drives A' and A" toward B' and B", thereby changing the angles of the rhombus. The usefulness of that is explained in the "equivalent circuit" in Fig. 7 where A' and A" have been compressed into A (and similarly for B, C and D) and we see that when A moves closer to B, then C and D must move further apart. The effect of this is that the large blocks to the right of C and left of D which are acting here like simple rigid members, also move away from the center and carry with them the points C and D. This is just what we want in order to avoid rotation at the hinges at F and G. It remains to get the right amount of sideways movement at C and D.

Consider the rhombus first. Let $AB=2q$, $CD=2p$ and let the side of the rhombus equal r . Then we have $q^2=r^2-p^2$ or $dp/dq=-q/p$ leading to

$$\Delta p = -\Delta q \frac{q}{p} = \frac{s}{2} \frac{AB}{DC} \quad (26)$$

where s is the sag of the mirror. Now consider the circle into which we are bending the mirror. The small angle θ at the end of the mirror is given by $\theta=L/2R_0$ and $s=(L/2)^2/2R_0$ therefore

$$\theta = \frac{4s}{L}. \quad (27)$$

The condition we really want to satisfy is

$$\frac{\Delta p}{u} = \theta \quad (28)$$

As a first step toward this we take the length of the mirror projected on the x -axis to be approximately constant. This is not strictly accurate but we will consider departures from it later. So substituting for Δp from (26) and for θ from (27) we arrive at

$$\frac{AB}{DC} = \frac{8u}{L} \quad (29)$$

which is the condition we are seeking. If we design the mechanism to obey this condition then we will have zero rotation of the hinges for all values of the sag. This conclusion does depend on the small-angle approximation but the latter is very well satisfied for cases of interest to us (θ normally less than a few milliradians). For simplicity we have discussed the progression from a sag, mirror curvature and end slope of zero toward some particular values s , $1/R_0$ and θ . However, this is not a necessary limitation. In view of the linear relationships among s , $1/R_0$ and θ , the above arguments would still hold for their increments in the event that s , $1/R_0$ and θ were being continuously tuned or had non zero values in the relaxed state of the mirror.

We now consider extension of the above reasoning to account for the end regions, which do not bend to the right radius, and the fact that the length of the mirror surface projected on the x axis may change as the mirror bends. The end regions are uniform beams each of length ΔL , and one can show that they bend by an angle exactly half the amount ($\Delta L/R_0$) that would have obtained had they followed the cube root prescription all the way to the end. It follows that this can be accounted for by inserting a factor $(1-\Delta L/L)$ on the right hand side of equation (29).

$$\frac{AB}{CD} = \frac{8u}{L} \left(1 - \frac{\Delta L}{L}\right). \quad (30)$$

The fractional change in length due to bending has a geometrical component equal to approximately $L^2/(12R_0^2)$ which is small in cases of practical interest. There is also a length change due the bending strain. This may not always be small but it is small at a depth below the mirror surface equal to the average depth \bar{h}_n of the neutral axis which is

$$\bar{h}_n = \frac{h_0}{2} \left[\frac{3}{4} \left(1 - \frac{2\Delta L}{L}\right)^{4/3} + \left(\frac{2\Delta L}{L}\right)^{4/3} \right]. \quad (31)$$

Fortunately, for cube-root mirrors with straight end sections, it is normally very convenient to place the effective hinge points at such a depth. Under these conditions we can then apply equation (29) directly

which allows the right shape for the rhombus to be determined and one can see that the ratio AB/CD will normally have values around 0.5-1 which are convenient to manufacture.

CONCLUSIONS

We have continued the analysis of monolithic adaptive x-ray mirrors begun in reference 1. We have calculated the torsional rigidities of various types of mirror and flexural hinge used in designing such devices allowing the systematic errors in the mirror surface due to hinge-induced torques to be evaluated. In many cases this understanding will allow sufficiently low-torque hinges to be designed by introducing straight sections in the center of the notch-type hinges. We have also shown how the bending properties of mirrors with cooling channels can be arranged to be the same as those without cooling channels. On the other hand for the most challenging cases where the hinge torques cannot be reduced sufficiently, we have proposed a new type of flexure design in which the hinge *rotations*, and hence also their torques, are reduced essentially to zero. We have analyzed the latter scheme and provided a simple prescription for choosing suitable design parameters.

ACKNOWLEDGEMENTS

The author is pleased to acknowledge helpful conversations with N. Andresen, F. Anthony, C. Corradi, W. Lowry, D. Lunt, W. McKinney, T. Tonneson and A. Warwick. This work was supported by the United States Department of Energy under Contract Number DE-AC03-76SF00098.

REFERENCES

1. M. R. Howells, D. Lunt, "Design for an Adjustable-curvature, High-power, X-ray Mirror Based on Elastic Bending", *Opt. Eng.*, **32**, 1981-1989 (1993).
2. Rockwell Power Systems, 2511C, Broadbent Parkway NE, Albuquerque, NM 87107, USA.
3. Photon Sciences International Inc., 210, South Plumer Ave, Tucson, AZ 85719.
4. G. E. Ice, C. J. Sparks, "A simple Cantilevered Mirror for Focussing Synchrotron Radiation", *Nucl. Inst. Meth.*, **A266**, 394-8 (1988).
5. R. J. Roark, *Formulas for Stress and Strain*, (McGraw-Hill, New York, 1964).

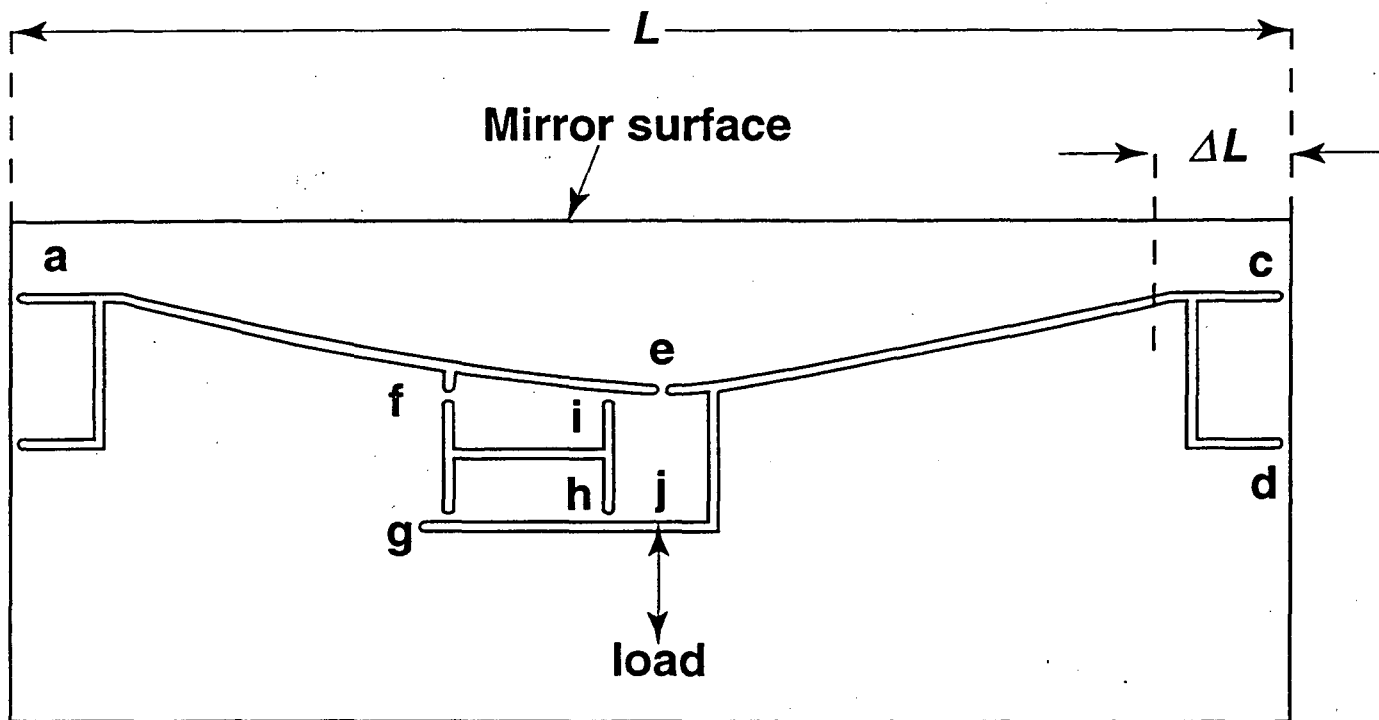
6. I. S. Gradshsteyn, I. M. Ryzhik, *Tables of Integrals Series and Products*, , (Academic Press, New York, 1980).
7. J. M. Paros, L. Weisbord, "How to Design Flexure Hinges", *Machine Design*, Nov 25, 1965.
8. S. Lindaas, "Compliance of Flexure Hinges", SUNY Stony Brook, Internal Report, (1991).
9. S. T. Smith, D. G. Chetwynd, D. K. Bowen, "Design and assessment of monolithic high precision translation mechanisms", *J.Phys. E*, 20 , 977-983 (1987).
10. N. Andresen, private communication.

FIGURE CAPTIONS

1. Basic design of a monolithic adaptive mirror from ¹. Note the link eif which prevents horizontal motion of the mirror center and the rectangle linkage fghi which constrains the member ej to move without rotation when driven. The hinges ab and cd ensure that temperature differentials between the mirror and the base do not lead to significant thermal stresses or changes in the mirror radius.
2. Geometry and notation for discussion of (a) flat-beam hinges, (b) double-sided notch hinges and (c) single-sided notch hinges.
3. The torsional rigidity of a double-sided notch hinge in ratio to that of a flat-beam hinge of the same parameters according to various forms of calculation. (a) full formula (equation (17)), (b)

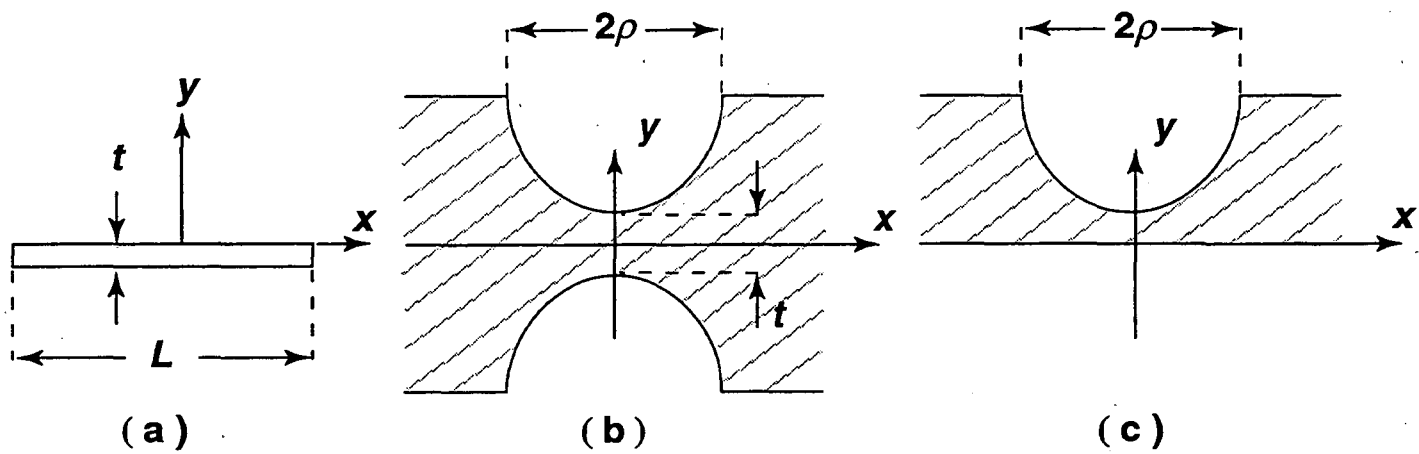
Paros-and-Weisbord approximate formula $G(y) = 16\sqrt{y}/3\pi$, (c) Smith-et-al finite element fit⁹, (d) (crosses) finite element calculations by Andresen¹⁰. The stress concentration factors (from Roark Table 37⁵, plotted as (e), are close to unity when the beam theory and finite element curves agree well and show departures from unity when they begin to disagree as one would expect.

4. Designs for composite hinges formed by joining a flat-beam hinge in series with two halves of a notch hinge. The purpose of such designs is to achieve a reduced torsional rigidity compared to a pure notch hinge without reducing the cross sectional area and hence the strength.
5. The factors by which the torsional rigidity of double-sided notch hinges is reduced by the introduction of straight sections in the center.
6. New type of adaptive mirror mechanism incorporating a system to cancel the rotations (and hence the error-producing torques) of all three of the hinges which connect to the mirror. The operating principle of the mechanism is explained in Fig. 7.
7. "Equivalent circuit" explaining the action of the rhombus mechanism at the center of the device shown in Fig. 6 where A' and A" have now been compressed into A (and similarly for B, C and D). When the mirror bends more concave, A and B move toward each other causing C and D to move away from each other. This moves point E to the right causing a small anti clockwise rotation of the link EF. The same change of mirror curvature also rotates the right hand end of the mirror anti clockwise and if the two rotations are arranged to be equal, (the prescription for which is explained in the text) then the hinge F will not rotate. This eliminates the hinge-induced distortions.



Xbl 947-5108

Fig. 1



Xbl 947-5109

Fig. 2

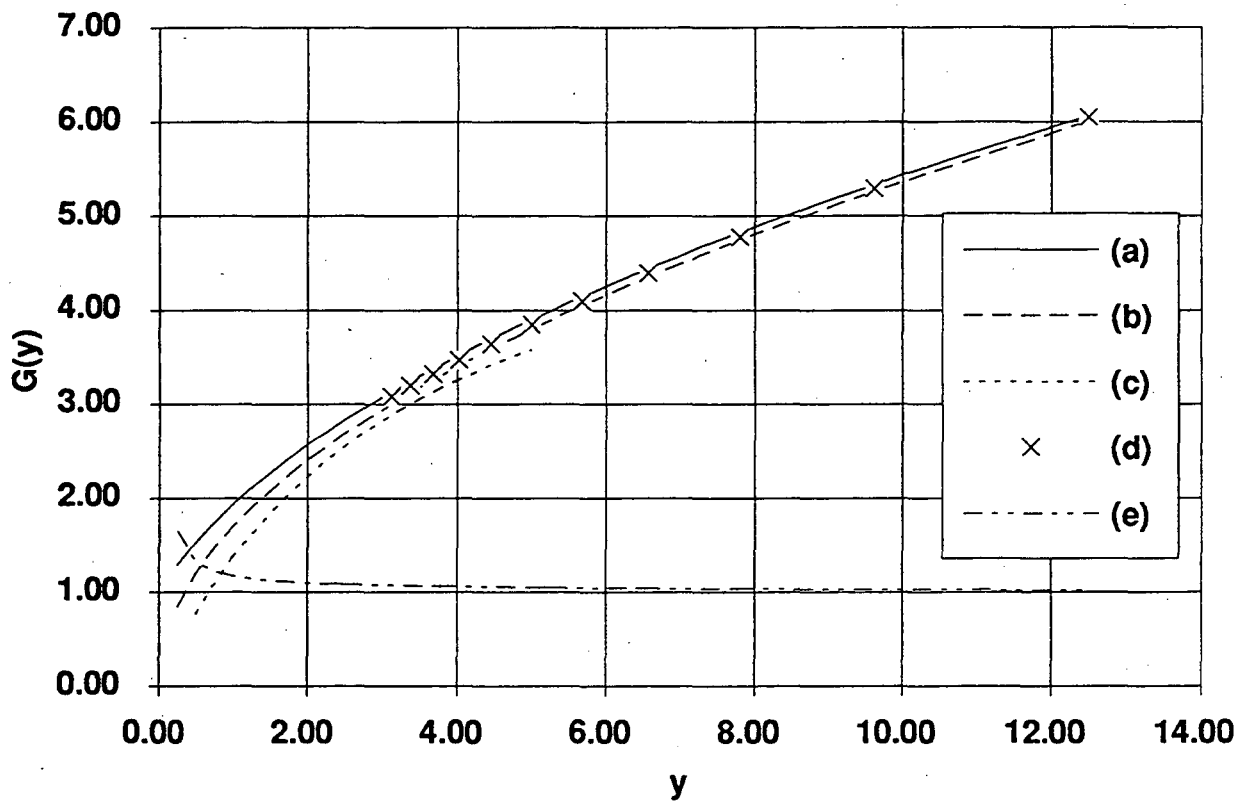
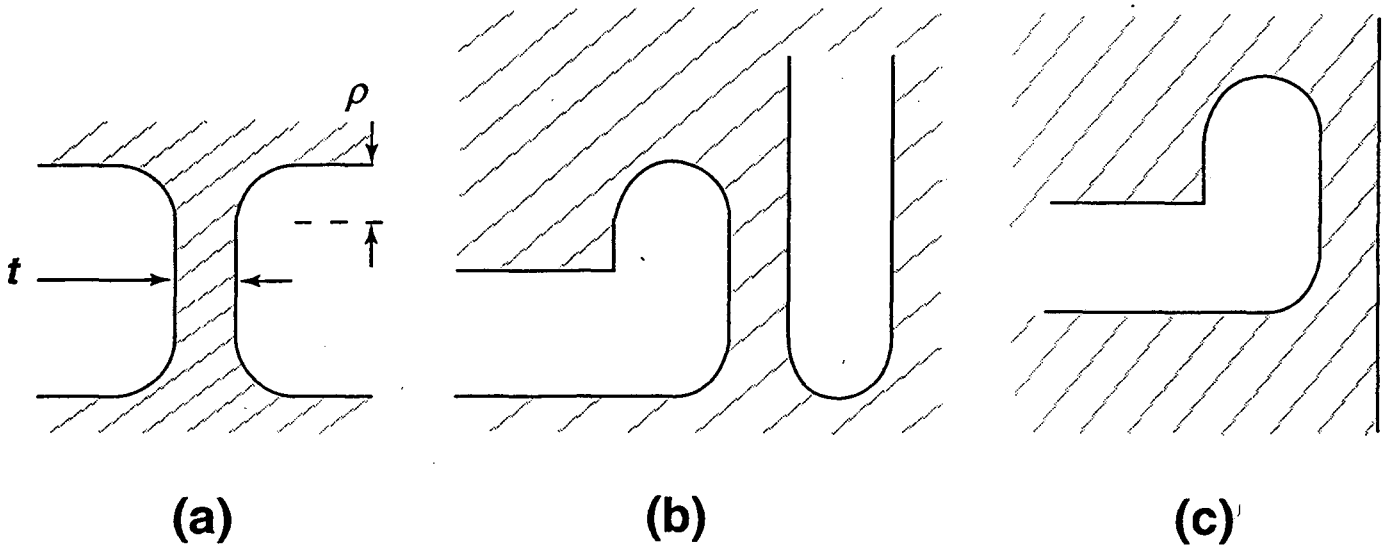


Fig. 3



Xbl 947-5111

Fig. 4

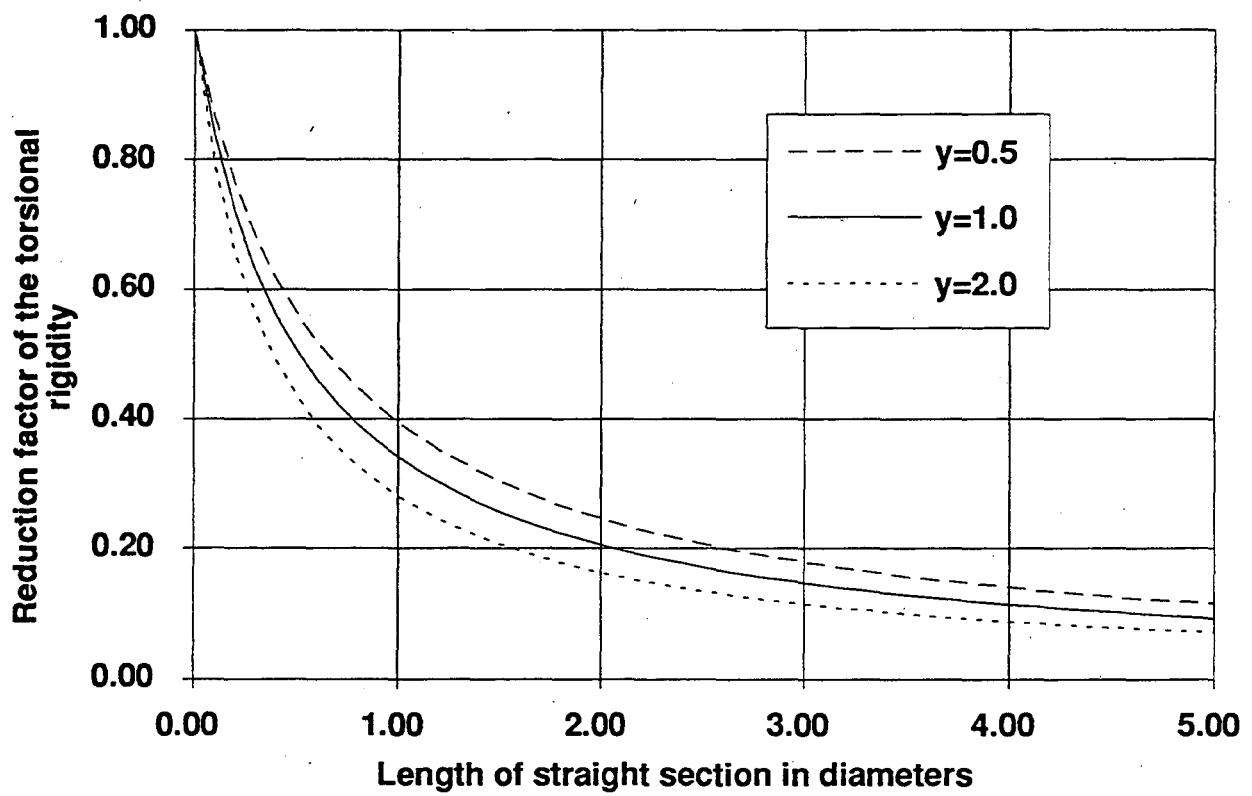
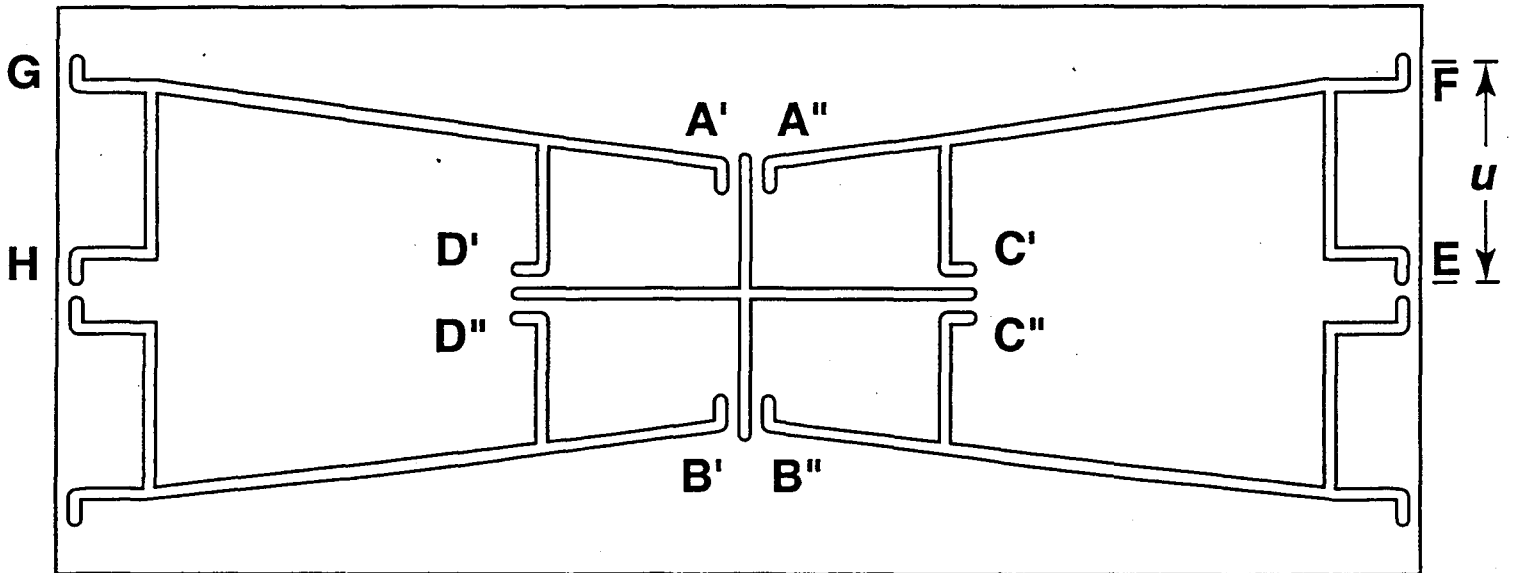
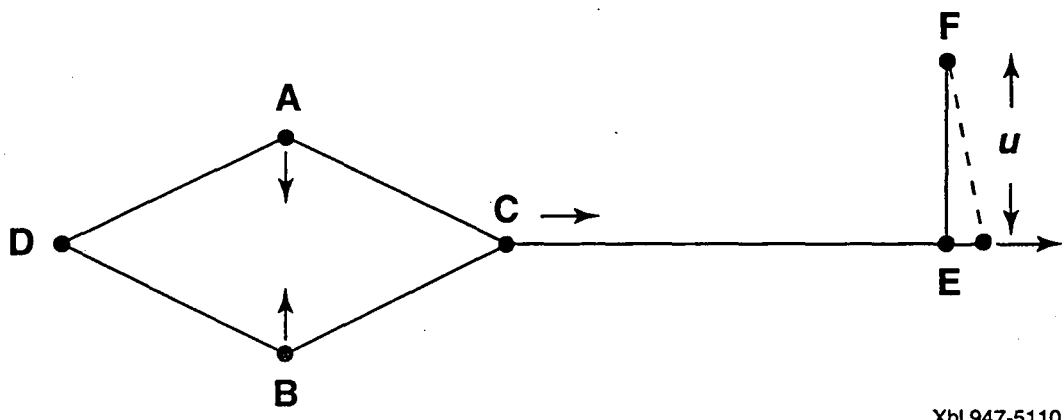


Fig. 5



Xbl 947-5112

Fig. 6



Xbl 947-5110

Fig. 7

LAWRENCE BERKELEY LABORATORY
UNIVERSITY OF CALIFORNIA
TECHNICAL INFORMATION DEPARTMENT
BERKELEY, CALIFORNIA 94720